METABOLICALLY INDUCED LIVER INFLAMMATION LEADS TO NASH AND DIFFERS FROM LPS or IL-1β-INDUCED CHRONIC INFLAMMATION

Wen Liang
Jan H. Lindeman
Aswin Menke
Debby Koonen
Martine Morrison
Louis M. Havekes
Anita M. van den Hoek
Robert Kleemann

Lab Invest. 2014; 94(5):491-502

ABSTRACT

Background & aims: The nature of the chronic inflammatory component that drives the development of non-alcoholic hepatosteatitis (NASH) is unclear and potential inflammatory triggers have not been compared to date. We tested the influence/effect of non-metabolic triggers (LPS, IL-1β, administered by slow-release minipumps) and metabolic dietary triggers (carbohydrate, cholesterol) of inflammation on the progression of bland liver steatosis (BS) to NASH.
Methods: ApoE3L.CETP mice fed a high-fat diet (HFD) developed BS after 10 weeks. Then, inflammatory triggers were superimposed or not (control) for 6 more weeks. Mouse livers were analyzed with particular emphasis on hallmarks of inflammation in human NASH. These hallmarks were defined in human liver biopsies with and without NASH.
Results: Livers of HFD-treated control mice remained steatotic and did not progress to NASH. All 4 inflammatory triggers applied activated hepatic NFκB significantly and comparably (⩾5-fold). However, HFD+LPS or HFD+IL1β did not induce a NASH-like phenotype and caused intrahepatic accumulation of almost exclusively mononuclear cells. By contrast, mice treated with metabolic triggers developed NASH, characterized by enhanced steatosis, hepatocellular hypertrophy and formation of mixed-type inflammatory foci containing MPO-positive granulocytes (neutrophils) as well as mononuclear cells, essentially as observed in human NASH. Specific for the metabolic inducers was an activation of the pro-inflammatory transcription factor AP-1, neutrophil infiltration, and induction of risk factors associated with human NASH, i.e. dyslipidemia (by cholesterol) and insulin resistance (by carbohydrate).
Conclusion: HFD feeding followed by NFκB activation per se (LPS, IL-1β) does not promote the transition from BS to NASH. HFD feeding followed by metabolically-evoked inflammation induces additional inflammatory components (neutrophils, AP-1 pathway) and causes NASH.

INTRODUCTION

Nonalcoholic fatty liver disease (NAFLD) is emerging as one of the most common liver disorders in modern societies (1). Its prevalence in the general population is strongly increasing together with obesity, dyslipidemia and the metabolic syndrome (2). NAFLD encompasses a range of conditions associated with accumulation of fat within liver cells. The most benign form of NAFLD is bland steatosis (BS), which is characterized by the accumulation of lipid droplets. BS can remain stable for many years and will never progress in many cases (1). In other cases BS does progress, leading to development of non-alcoholic steatohepatitis (NASH), which is characterized by fat accumulation and inflammation. This condition is not benign and can further progress to liver fibrosis and cirrhosis with high rates of morbidity and mortality (3, 4). The factors that trigger this transition from BS to NASH are unknown.

The pathogenesis of NASH is thought to be driven by a lipid component and an inflammatory component (2, 5). Excessive intrahepatic fat accumulation may sensitize the liver to subsequent inflammatory insults that promote the development of NASH. The exact nature of these inflammatory insults or 'second hits', viz. the mechanism inducing the inflammatory component of the disease, is largely unclear (6). The pro-inflammatory transcription factor NFκB may critically influence this process and chronic activation of NFκB is associated with many pathogenic liver conditions (7). A causal role for hepatic NFκB in the progression of BS to NASH has been proposed recently in transgenic mice selectively expressing constitutively active IKKβ in hepatocytes (8). Among the inflammatory triggers that may be responsible for chronic activation of NFκB in liver cells are circulating endotoxins (LPS) or pro-inflammatory cytokines such as interleukin-1beta (IL-1β) (9, 10). However, low-grade hepatic inflammation may also be evoked by other types of stimuli such as unhealthy diets or excess eating, which represent metabolic triggers of inflammation that may activate multiple pathways simultaneously (11, 12). For instance, diets with a high content of metabolizable energy from carbohydrate or diets rich in cholesterol can cause chronic activation of NFκB in the liver (6, 12-15).

In this study we tested the influence of different inflammatory triggers with NFκB-activating properties on the transition of BS to NASH and analyzed whether disease progression depends on the type of trigger employed. More specifically, we compared the effects of non-dietary inflammatory stimuli (LPS, IL-1β) and diet-related metabolic inflammatory stimuli (carbohydrate, cholesterol) all of which were superimposed on a high-fat diet (HFD) in separate groups of mice. Transgenic ApoE3*Leiden.huCETP (E3L.CETP) mice were used because their lipoprotein metabolism is translational to the human situation and these animals are prone to develop obesity, dyslipidemia and NAFLD on HFD (16, 17). Chronic exposure to low concentrations of LPS and IL-1β was achieved by minipump technology, and metabolically evoked inflammation was induced by feeding diets rich in carbohydrates or cholesterol. Prior to analysis of experimental NASH, human liver biopsies with and without NASH were analyzed to define hallmarks of inflammation of human NASH. Combined histological and biochemical analysis of mouse livers resulted in identification of cellular and molecular determinants that are crucial for the transition of BS to NASH.

MATERIALS AND METHODS

Human liver biopsies

Human liver biopsies were obtained at autopsy for postmortem histological analysis by pathologists (Department of Pathology; Leiden University Medical Center/LUMC, Leiden, The Netherlands). N=21 specimens with NASH and n=12 control subjects without NASH were used for this study (diagnosed by pathologist). Tissue was obtained and handled in accordance with the guidelines set by the LUMC medical ethical committee. Cardiovascular disease was the predominant cause of death. In all, 40% of the subjects were female and 60% male. The average age was 62 years. Cross-sections were stained with anti-MPO (A0398, Dako, Glostrup, Denmark) and phospho-p65-NFκB (#3037, Cell Signaling, Danvers MA, USA) as described (18).

Animals and diets

Male ApoE*3-Leiden.huCETP transgenic mice (E3L.CETP) were 10-14 weeks old and obtained from an in-house breeding colony (TNO Metabolic Health Research) (18). Briefly, ApoE*3-Leiden were crossed with hemizygous human CETP transgenic mice and offspring was genotyped using the primers CETP-F sequence: GAATGTCTCAGAGGACCTCCC, CETP-R sequence: CTTGAACTCGTCTCCCATCAG; ApoC1-L sequence: GGTCCCGGGCACTTCCC TTAGCCCCA; ApoC1-R sequence: TTTGAGCTCGGCTCTTGAGACAGGAA. Furthermore, presence of human ApoE3 protein and human CETP protein in plasma was confirmed by ELISA.

Experiments were approved by an ethical committee on 'Animal care and Experimentation', Zeist, The Netherlands. Mice were kept on chow diet (Ssniff R/M-H, Ssniff Spezialdiäten, Soest, Germany) until the start of the experiment. Animals had free access to water and diet during the study period of 16 weeks. The group size was n=9-10. One group remained on chow and served as aging control. The other animals received a high-fat diet (HFD; 24% w/w lard, Research Diets, New Brunswick NJ, USA) for 10 weeks (run-in) and were then matched into groups based on total plasma cholesterol, triglycerides and body weight. HFD feeding was continued in all groups. Groups were additionally treated with one of the following treatments until week 16: LPS from Salmonella minnesota R595 (Lot#30446A1, List-Biological Laboratories, Campbell CA, USA) by minipump at 5 µg/day; recombinant murine IL-1β (Lot#030447, PeproTech, Rocky-Hill NJ, USA) by minipump at 100 ng/day; dietary carbohydrate (Ensure® Plus in drinking water, Abbott Laboratories, Hoofddorp, The Netherlands); dietary cholesterol (1% w/w mixed into HFD) (Sigma-Aldrich, Zwijndrecht, The Netherlands). Osmotic minipumps (Alzet, Lot#10194-08, Maastricht, The Netherlands) were placed subcutaneously in the back region (flow-rate: 0.10 µL/hour, 101 µL total volume) under isoflurane anesthesia. Two controls groups were included; they were treated with either HFD+PBS (minipump) or HFD only. These groups were comparable in all histological scores and were therefore analyzed as one.

Histological and biochemical analysis

The right median liver lobe (lobus dexter medialis hepatis) was carefully isolated, fixed in 4% paraformaldehyde (2 days), embedded in paraffin and cross-sectioned (5 µm). The other

liver lobes were snap-frozen and stored at -80°C. Hematoxylin-eosin (HE)-stained cross-sections were scored blindly by a pathologist using an adapted grading method for human NASH (19) with specific emphasis on hallmarks of steatosis and inflammation. Briefly, two cross-sections were examined per mouse and the level of vacuolization was determined relative to the total liver area analyzed, i.e. expressed as a percentage. The extent of vacuolization was scored as 'Slight' (<5%), 'Moderate' (5-33%), 'Severe' (34-66%) and 'Very Severe' (>66%). Of note, hepatocellular ballooning (central nucleus, web-like structure in cytoplasm) is a hallmark of human NASH but mouse livers merely show enlarged hepatocytes containing small intracellular lipid droplets, herein referred to as 'hepatocellular hypertrophy'. The extent of enlarged hepatocytes (diameter >1.5 normal) was analyzed using the same percentage categories as for vacuolization to provide quantitative information about abnormally enlarged cells. Inflammation was scored by counting and analyzing the type of inflammatory cells (mononuclear and/or polymorph nuclear) in a defined area of five random microscopic fields per animal. Inflammation was graded as 'Normal' (<0.5 foci), 'Slight' (0.5-1.0 foci), 'Moderate' (1.0-2.0 foci), 'Severe' (>2.0 foci). Collagen was stained using Picro-Sirius red staining (Sigma-Aldrich).

Liver lipids

The intrahepatic concentration of free cholesterol, triglycerides and cholesteryl esters was analyzed as described (20). Briefly, 200 µg of frozen liver biopsies were homogenized in MilliQ H_2O and the protein content was determined. Two µg of cholesterol acetate was added to each sample as an internal standard. Lipids were extracted using methanol and chloroform. Extracted lipids were then separated by thin layer chromatography using a silica-gel-60 pre-coated plate. Plates were incubated at 130°C for 30 min and band densities were then quantified (20). In addition, cryostat-sections were stained with Oil-Red O (Sigma-Aldrich) to identify lipids, and counterstained with hematoxylin (Sigma-Aldrich) to visualize nuclei.

Immunohistochemical staining

Paraffin-embedded liver cross-sections were used for analysis of MPO-positive cells (neutrophils) using anti-MPO (ab9535-Abcam, Cambridge, UK). After pre-treatment with target retrieval solution (3-in-1; Dako) at pH 9.0, cross-sections were incubated with primary anti-MPO overnight. Sections were peroxidase blocked in 3% H_2O_2 in methanol for 10 minutes and detected with Dako Envision-Flex amplification kit (Product#K800021). For analysis of CD11b, frozen liver samples were used. After fixation with acetone, cross-sections were incubated with anti-CD11b (Lot#ab8878, Abcam) for one hour followed by incubation with biotinylated rabbit anti-rat antibody (Lot#00065538, Dako). Immunoreactivity was visualized with streptavidin/HRP (Lot#00057815, Dako) and AEC (Lot#10043262, Dako). For all IHC analyses, negative controls were performed by omitting the primary antibody.

Analysis of transcription factor activity in liver homogenates

To determine the amount of activated p65-NFκB, AP-1, STAT3 and C/EBP-β protein in livers, protein extracts were prepared using a Nuclear Extract Kit (Cat.#40010, ActiveMotif, Rixensart, Belgium). The protein content of the extracts was determined with Bio-Rad dye

reagent (Cat#500-0006, Bio-Rad Laboratories-GmbH, Munich, Germany). Six µg of protein was used for transcription factor activity analysis using TransAM® kits for NFκB-p65 Chemi, c-Jun, STAT3 and C/EBP-β kits (Cat.#40097, 46096, 45196, 44196, ActiveMotif) as reported (11, 20). Briefly, the amount of active transcription factor was determined by measuring its binding capacity to a consensus binding sequence in presence of a competitor oligonucleotide or a mutant (non-competitor) oligonucleotide to control for the specificity of DNA binding. Data are provided as relative units.

Plasma parameters, lipoproteins and plasma inflammatory markers

EDTA (Sarstedt, Numbrecht, Germany) plasma was collected after a 5-hour fast (8 am to 1 pm). Plasma levels of glucose (Instruchemie, Delfzijl, The Netherlands), insulin (Mercodia, Uppsala, Sweden), total cholesterol and triglycerides (Roche Diagnostics, Almere, The Netherlands) were measured with commercial kits. HOMA index was calculated according to the formula HOMA = fasting plasma glucose (mM) x fasting plasma insulin (ng/mL)/22.5. Lipoprotein profile analysis was performed with AKTA-FPLC (18). The plasma levels of E-selectin and SAA were determined by ELISA (R&D-Systems, Abington, UK for E-selectin, Life Technologies, Bleiswijk, the Netherlands for SAA). Plasma ALAT activity was measured using a Reflotron® kit (Roche Diagnostics).

Statistics Analysis

Statistical analyses were performed with StatView software (SAS-Institute, Cary, NL), and a P-value <0.05 was considered statistically significant. Differences between groups were analyzed using Mann-Whitney non-parametric test for two independent samples. The data obtained from histological scoring of livers were analyzed using 2-sided Fisher's exact test. All values shown represent means ± SEM.

RESULTS

Characterization of the inflammatory component in human NASH

HE-stained human tissue biopsies were analyzed for steatosis and inflammation. Livers of patients with NASH showed pronounced vacuolization compared with controls (**Figure 1A/B**). Quantitative analysis revealed that about 40% of the surface area was steatotic (P<0.001 versus control; **Supplementary Material-A**) of which 35% was macrovesicular steatosis and 5% microvesicular steatosis. Hepatocellular ballooning was observed in NASH livers but not in controls (**Figure 1A/B**). Also, enlarged hepatocytes containing small lipid droplets were observed in NASH specimens only (**Supplementary Material-B**). NASH livers were characterized by lobular inflammation, i.e. an abundant presence of mononuclear cells and polymorph-nuclear leukocytes (granulocytes) which formed foci (**Figure 1A/B**). Inflammatory cell foci contained CD68-positive cells of the monocytes/macrophage lineage (not shown) as well as granulocytes with MPO-positive immunoreactivity (neutrophils), a hallmark of human NASH (**Figure 1C/D**). NASH livers also showed a pronounced expression of p65-NFκB (in inflammatory foci and steatotic areas), while only a few p65-NFκB-positive cells were observed in healthy control livers

(**Figure 1E/F**). Fibrosis was present in most (73%) human NASH specimens, and in none of the controls (**Figure 1G/H**).

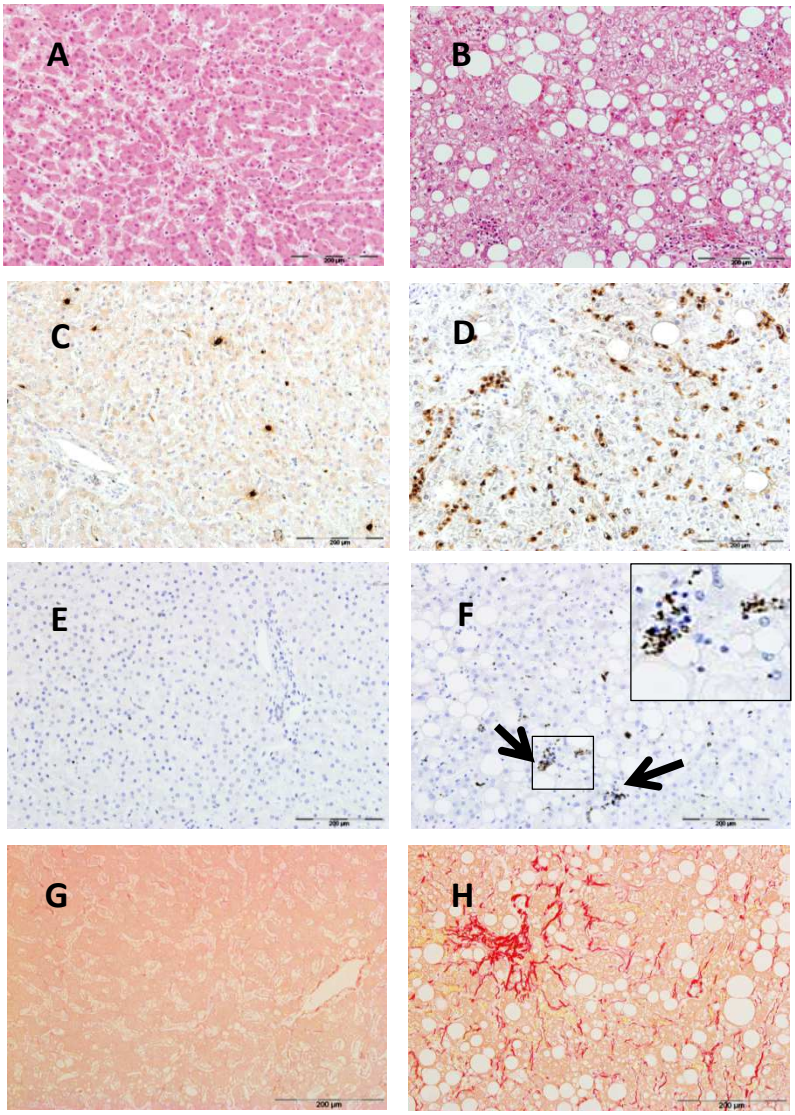

Figure 1: Analysis of inflammation in human NASH. Representative photographs of control livers (n=12, panels left) were compared to NASH specimens (n=21, panels right). (A/B) HE staining showed pronounced vacuolization in NASH livers which was associated with inflammatory cell aggregates (solid arrow) and hepatocellular ballooning (magnified in insert). (C/D) Immunostaining showed inflammatory cell foci (arrows) containing myeloperoxidase (MPO)-positive cells in NASH. (E/F) Immunostaining of p65-NFκB-positive cell clusters (arrows) in NASH (magnified in insert). (G/H) Picro Sirius red staining demonstrated NASH with fibrosis in 15 out 21 specimens.

Effects of HFD feeding and addition of inflammatory triggers on the development of experimental NASH

To gain insight into the nature of the inflammatory trigger that may underlie the development of BS into NASH, we evaluated the effects of different inflammatory stimuli superimposed on HFD feeding. Treatment with inflammatory stimuli was started after a 10-week run-in period on HFD, which resulted in BS and moderate pericentral hepatocellular vacuolization (**Supplementary Material-C**). Lobular inflammation was not observed after 10 weeks of HFD run-in.

HFD feeding was continued for six more weeks and experimental groups additionally received either PBS (minipump control), LPS (minipump), IL-1β (minipump), dietary carbohydrate (Ensure®) or dietary cholesterol. A second control group was continued on HFD only. A separate group was fed chow during the complete experimental period (16 weeks) and served as a reference. All interventions were well-tolerated and the superimposed inflammatory triggers did not affect the daily food intake relative to HFD control, i.e. calorie intake was comparable between the groups (on average 12 kcal/day per animal) except for the HFD+carbohydrate group (16 kcal/day per animal). At sacrifice, livers were immediately prepared for histological examination and biochemical analysis of active p65-NFκB. Representative photomicrographs of livers are shown in **Figure 2A-F**. Reference mice on chow had normal livers without steatosis or inflammation (**Figure 2A**). The two control groups, i.e. HFD feeding alone and HFD+PBS-minipump treatment, were comparable and showed moderate steatosis with vacuolization of the pericentral zone and the midzone as well as hepatocellular hypertrophy (individual data provided in **Supplementary Material-D**). Livers of these groups hardly contained inflammatory foci, demonstrating that HFD feeding *per se* is not sufficient to induce a NASH-like phenotype within a period of 16 weeks (**Figure 2B**).

Consistent with the low abundance of cellular inflammation in HFD-treated mice, the level of transcriptionally active p65-NFκB protein measured by TransAM® was very low (1.1×10^5 relative units, RLU) (**Figure 3A**). Treatment with the inflammatory triggers LPS, IL-1β, carbohydrate and cholesterol resulted in significantly higher levels of activated p65-NFκB protein in mouse livers. The p65-NFκB activating effects of the different inflammatory stimuli were statistically comparable. This demonstrates that p65-NFκB was activated at least 5-fold or more in liver at the end of the study relative to HFD alone.

Histological analysis of experimental NASH allowed quantification of the effects of the different inflammatory triggers on vacuolization, hypertrophy and inflammation compared with HFD alone (**Figure 3A-C**; individual histological scores see **Supplementary Material-D/E**). Chronic exposure to LPS did not further aggravate vacuolization and hypertrophy relative to HFD control (**Figures 2C** and **3B/C**). The inflammatory cell content of LPS-treated animals was higher than in controls treated with HFD only. Inflammatory cells were mainly mononuclear and diffusely distributed, and polymorph nuclear cells were hardly observed. Surprisingly, livers of mice treated with IL-1β showed even less

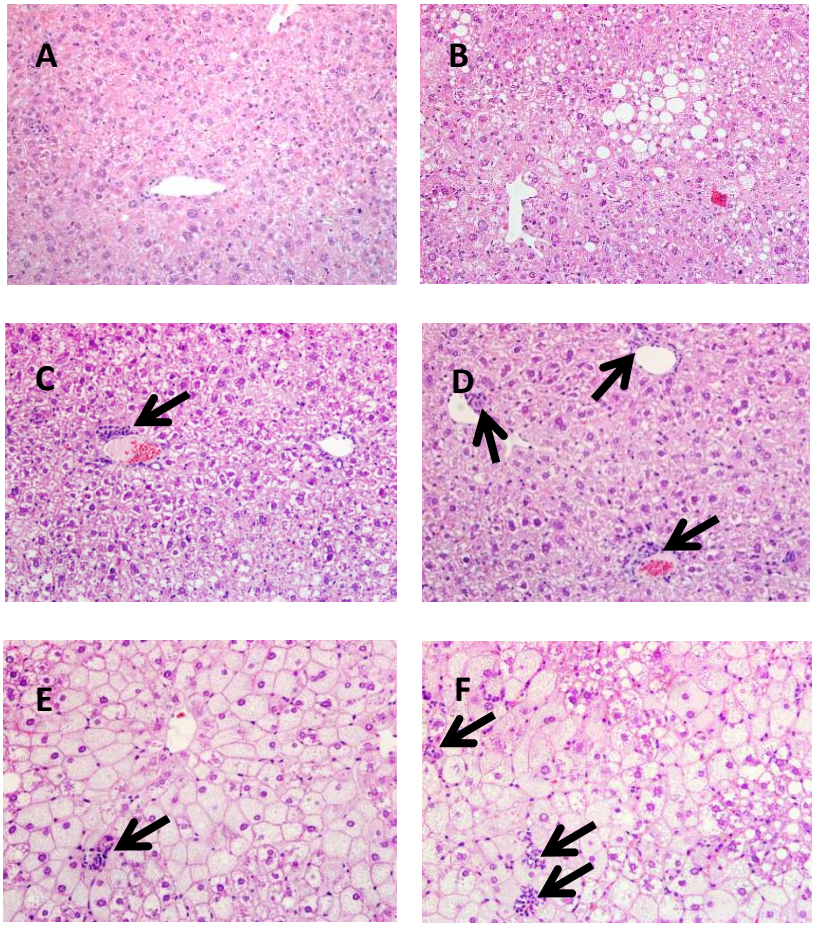

Figure 2: Histological presentation of experimental NASH. Representative photomicrographs are shown at 200-fold magnification. Mice were treated with (A) chow (reference group), (B) HFD (control group) and HFD plus additional inflammatory stimuli (C) LPS, (D) IL-1β, (E) dietary carbohydrate and (F) dietary cholesterol. Inflammatory infiltrates are indicated with arrows.

vacuolization than HFD control mice (**Figure 2D** and **3B**). Hepatocellular hypertrophy was not observed with IL-1β. Similar to LPS, the inflammatory cell content was higher than in HFD controls, but again inflammatory cells were predominately of the mononuclear type and diffusely distributed across the liver. Inflammatory cell foci were frequently found in close proximity to vascular structures.

In contrast to LPS and IL-1β, the metabolic stimuli (carbohydrate and cholesterol) clearly promoted the development of a NASH-like phenotype and resulted in pronounced changes in shape and size of hepatocytes: Carbohydrate-treated animals showed

pronounced micro-vacuolization and enlarged hepatocytes containing small lipid droplets, also in the periportal zone, which was not affected in HFD control livers (**Figure 2E** and

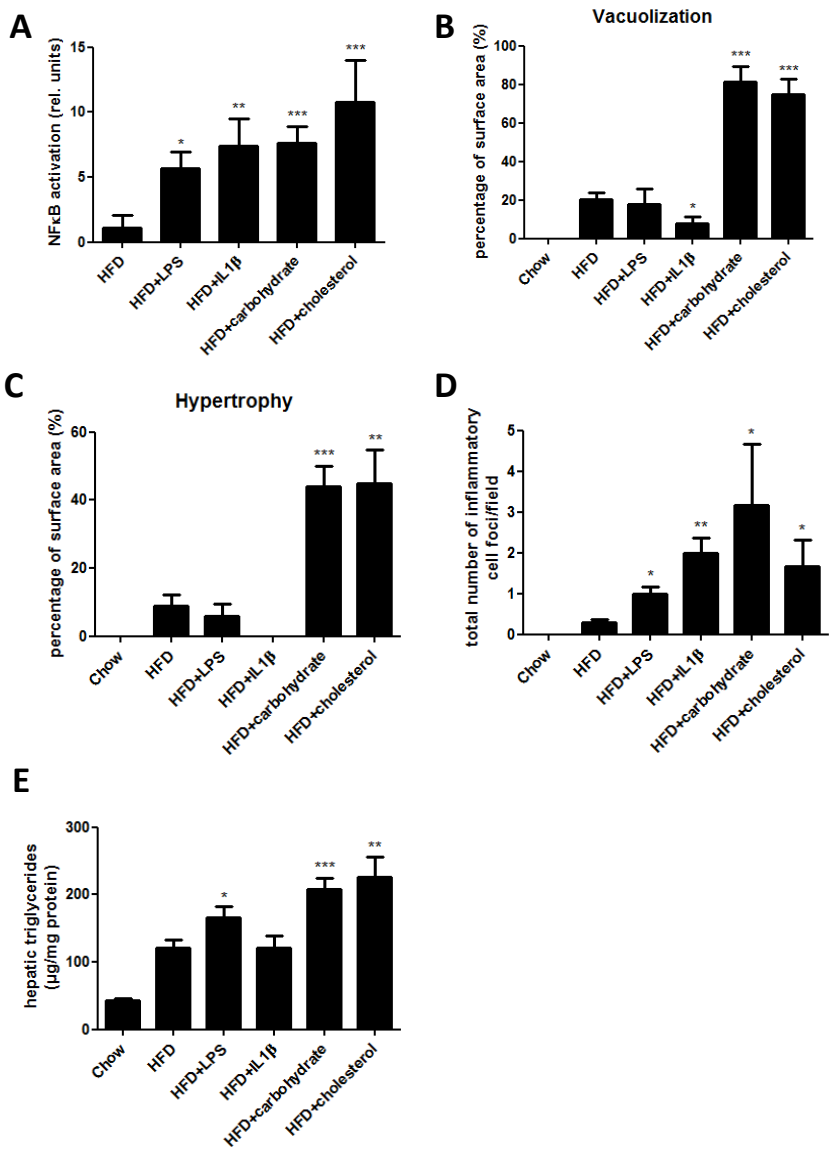

Figure 3: Quantitative analysis of experimental NASH. Quantification of (A) activated p65-NFkB measured by TransAM® in liver homogenates, (B) vacuolization and (C) hepatocellular hypertrophy as percentage of the total liver area analyzed (%). (D) Number of inflammatory foci per microscopic field. (E) Quantitative analysis of the intrahepatic triglycerides. Groups treated with inflammatory stimuli are compared to HFD control. *P<0.05, **P<0.01, ***P<0.001.

Supplementary Material-D). Quantification of hepatocellular vacuolization and hypertrophy revealed that carbohydrate feeding increased these parameters significantly and about 4-fold ($P<0.05$) relative to HFD (**Figure 3B/C**). Mixed-type inflammatory cells (i.e. mononuclear and polymorph nuclear cells) were present and inflammatory cell foci were observed.

Cholesterol-treated livers resembled carbohydrate-treated livers and also showed extensive micro and macro-vacuolization with large vacuoles in pericentral and periportal zones. Livers had a significantly increased content of inflammatory cell foci (**Figure 2F**). The effects of cholesterol on vacuolization, hypertrophy and inflammation were all significant (**Figure 3B-D**) and statistically comparable to the effect of the other metabolic trigger, carbohydrate.

Biochemical analysis of the intrahepatic triglyceride concentrations (**Figure 3E**) and parallel Oil Red O staining (not shown) were in line with the histological analyses and confirmed that only the metabolic triggers, carbohydrate and cholesterol, promoted a transition of BS to NASH. Most of the mice did not develop fibrosis within the study period: only one mouse (cholesterol treated group) did develop NASH with fibrosis (Sirius red collagen staining, not shown).

Effect of non-metabolic and metabolic inflammatory triggers on inflammatory cells and inflammatory pathways

Experimental livers were further analyzed histologically and biochemically to identify determinants that distinguish the metabolic triggers from LPS and IL-1β. A more refined histological analysis of inflammatory cells present in liver revealed that LPS and IL-1β treatment led to an almost exclusive recruitment of mononuclear cells; whereas carbohydrate and cholesterol treated livers contained mixed-type inflammatory cells including polymorph nuclear cells (**Figure 4G**). Consistent with this observation, more MPO-positive cells (neutrophils) were observed in the groups exposed to carbohydrate or cholesterol but not in those treated with LPS or IL-1β (**Figure 4A-F**). Immunohistochemical analysis of the monocyte/macrophage marker CD68 revealed no difference among the experimental groups, except a slight increase in the IL-1β-treated (1.5-fold) and cholesterol-treated (2-fold) groups (not shown). Furthermore, the number of Mac1/CD11b-positive cells did not differ between the groups (not shown). Together, this shows that an abundant presence of neutrophils, a hallmark of human NASH, discriminates the two metabolic inflammatory triggers from the two non-dietary triggers (LPS and IL-1β).

To gain more insight into the molecular effects of the different triggers we analyzed transcription factor activity downstream of specific inflammatory pathways by TransAM® technology. Independent of the type of inflammatory trigger, the activity of C/EBP-β tended to be lower than in HFD controls (**Supplementary Material-F**). The transcriptional activity of STAT3 was slightly increased in the LPS- and IL-1β-treated groups but the effects did not reach statistical significance (**Supplementary Material-G**). Treatment with carbohydrate and cholesterol significantly increased the transcriptional activity of AP-1, an effect that differentiated the metabolic triggers from LPS and IL-1β (**Figure 4H**). With respect to systemic markers of inflammation, plasma E-selectin levels were increased by

IL-1β and plasma SAA levels were increased by IL-1β, carbohydrate and cholesterol treatment (**Table 1**).

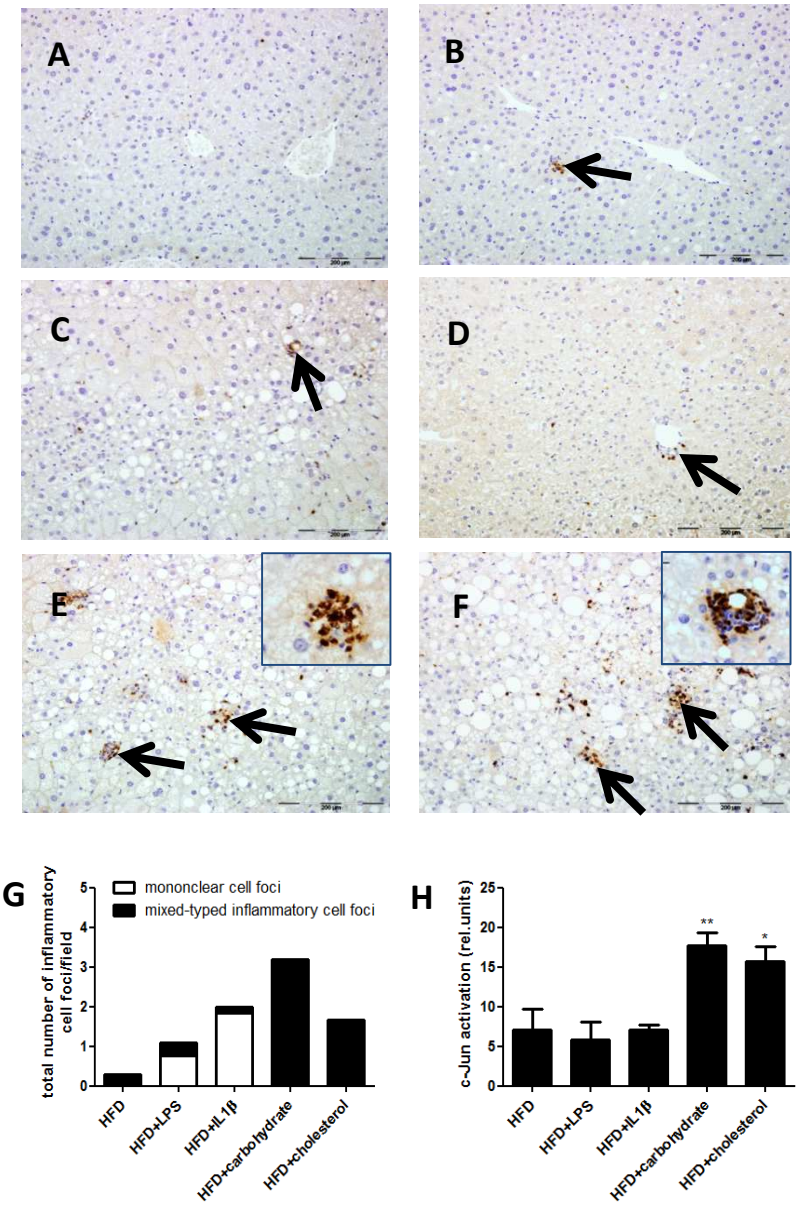

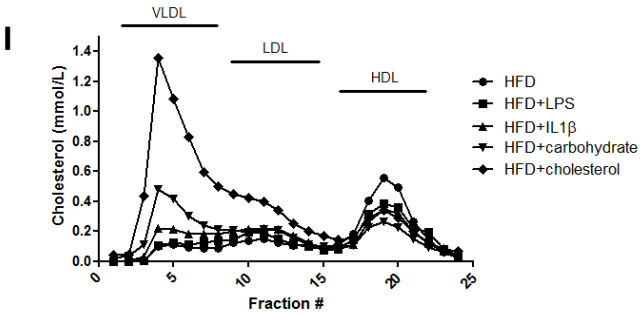

Figure 4: Characterization of inflammation in experimental NASH. Immunohistochemical staining of MPO in (A) chow reference, (B) HFD control and HFD plus (C) LPS, (D) IL-1β, (E) carbohydrate or (F) cholesterol. Inflammatory cell foci (arrows) containing MPO-positive cells. (G) Relative contribution of mononuclear cell foci and mixed-type inflammatory cell foci to the overall content of inflammatory cells for each group (H) Transcriptional activity of c-Jun (a subunit of AP-1) protein by TransAM® analysis. (I) Lipoprotein profile at t=16 weeks. *P<0.05, **P<0.01.

Table 1: Experimental treatments have a differential effect on risk factors of NASH. Parameters shown were determined in fasting plasma at the end of the experimental period (week 16). Intrahepatic lipids were determined in freshly prepared tissue homogenates. Values are means ± SEM. Significance is indicated *P<0.05, **P<0.01, ***P<0.001 versus HFD control (Mann-Whitney test).

	HFD	**HFD + LPS**	**HFD + IL1β**	**HFD + carbohydrate**	**HFD + cholesterol**
Body weight [g]	**39.9**±0.9	**39.9**±1.5	**37.3**±2.0	**47.6**±1.2***	**42.1**±2.0
Visceral fat [g]	**0.7**±0.1	**0.7**±0.1	**0.7**± 0.1	**1.1**±0.1**	**0.7**±0.1
Cholesterol [mM]	**4.7**±0.3	**4.2**±0.3	**4.8**±0.4	**6.5**±0.6*	**16.2**±2.0***
Triglycerides [mM]	**1.4**±0.3	**1.6**±0.2	**2.1**±0.3*	**4.3**±0.6***	**3.4**±0.7**
Fasting glucose [mM]	**13.5**±0.9	**13.3**±0.6	**10.9**±0.9*	**17.2**±0.8**	**14.4**±0.7
Insulin [ng/mL]	**1.15**±0.3	**1.37**±0.3	**2.41**±0.6	**4.28**±0.9**	**1.15**±0.3
Intrahepatic free cholesterol [µg/mg protein]	**14.1**±0.7	**16.6**±0.9*	**14.5**±0.7	**17.2**±0.9*	**20.1**±1.6**
Intrahepatic cholesterol ester [µg/mg protein]	**12.8**±0.8	**14.5**±1.5	**12.4**±1.4	**20.4**±2.9*	**48.0**±4.0***
ALAT [U/L]	**76**±16	**76**±22	**59**±15	**176**±66*	**151**±41
E-selectin [ng/mol]	**30**±7	**33**±1	**66**±2***	**31**±1	**31**±1
SAA [µg/mL]	**5.03**±1.30	**5.30**±1.67	**37.8**±14.2**	**6.7**±2.2*	**14.5**±4.6**

Effect of non-metabolic and metabolic inflammatory triggers on risk factors associated with NASH

Table 1 shows data of risk factors that are typically associated with NASH development in humans, e.g. body weight, visceral fat mass, plasma lipids, fasting glucose and insulin, and ALAT. These risk factors were not affected by LPS. IL-1β treatment also did not affect these parameters, except a slight increase in triglycerides and a decrease in glucose. In contrast, the metabolic triggers worsened risk factors that are typically associated with

NASH development in humans. Carbohydrate treatment resulted in an increased body weight (47.6 ± 1.2 g; P<0.001) and visceral fat mass (1.1 ± 0.05 g; P<0.01) beyond that of HFD controls. Also, plasma cholesterol and triglyceride concentrations were significantly higher in carbohydrate-treated animals. Increased fasting plasma glucose (17.2 ± 0.8 mM; P<0.01) and insulin (4.28 ± 0.9 ng/mL; P<0.05) levels indicated insulin resistance ($HOMA_{carbohydrate}$= 3.3 versus $HOMA_{HFD\ control}$= 0.9). Treatment with cholesterol had a marked adverse effect on plasma cholesterol and triglycerides and little effect on the other risk factors. Also, intrahepatic free cholesterol and cholesterylester levels were increased. Lipoprotein profile analysis revealed that the observed increase in plasma cholesterol was confined to VLDL/LDL-sized particles. All treatment groups showed a relative decrease in HDL compared to HFD control animals (**Figure 4I**). Plasma ALAT levels were only elevated in the groups treated with metabolic inflammatory triggers.

DISCUSSION

There is ample evidence that development of NASH is driven by chronic inflammation but the nature of the inflammatory component is not very clear (1-5, 21), and possible inflammatory triggers have not been investigated systematically. The present study examined the influence of metabolically evoked inflammation (carbohydrate, cholesterol) and non-metabolic inflammatory triggers (LPS, IL-1β) on the development of experimental NASH. Herein, we present the first head-to-head comparison of these triggers, revealing that they differ in their potency to stimulate progression of steatosis and induction of NASH. Only the metabolic triggers aggravated steatosis and led to an infiltration of neutrophils as well as activation of AP-1, a hallmark of lipotoxicity (22). Furthermore, they induced metabolic risk factors (insulin resistance, dyslipidemia) associated with NASH development in humans, which were not observed for the non-metabolic triggers.

The HFD control group that remained on HFD during the complete experimental period did not show inflammatory cell infiltrates, had low AP-1 and NFκB levels and did not progress from steatosis to NASH. Treatment with metabolic or non-metabolic inflammatory triggers activated hepatic NFκB significantly and comparably. Despite this clear pro-inflammatory effect in liver, LPS and IL-1β-treated mice did not progress to NASH. Thus, simultaneous HFD feeding and activation of hepatic NFκB *per se* in livers with established steatosis is not sufficient to induce NASH development, indicating that additional inflammatory factors or pathways are involved. Livers of LPS and IL-1β-treated groups exhibited cell infiltrates consisting almost exclusively of mononuclear cells, with hardly any mixed-type infiltrates, a characteristic feature of biopsy-proven human NASH (21). The selective effect of endotoxin on recruitment of mononuclear cells is in line with human and rodent studies in which elevated LPS activity in serum was associated with macrophage-mediated chronic inflammation and increased levels of monocyte chemoattractant protein-1 (23, 24). Thus, chronic LPS and IL-1β exposure may merely activate and recruit specific populations of inflammatory cells to liver and the absence of neutrophil infiltrates indicates these triggers by themselves do not cause hepatocellular damage. Consistent with this notion we observed no increase in ALAT when mice were treated with LPS or IL-1β. Hence, administration of LPS and IL-1β by minipump constitutes

an ‘exogenous’ form of inflammation while the two metabolic triggers employed herein affect liver metabolism (20) and ‘endogenous’ inflammatory processes related to it (12, 14), possibly causing liver damage. Lipotoxicity and/or the relatively high levels of free cholesterol observed in these groups may constitute causes of liver damage.

Neutrophil infiltration is an important hallmark of biopsy-proven NASH in humans (21) that distinguishes subjects with NASH from those without, independent of obesity (25). It is not clear whether neutrophils are innocent bystanders or causally involved in the pathogenesis, and investigators have only recently begun to characterize the role of neutrophils in NAFLD. The molecular mechanisms that allow neutrophils to home to the liver are also not well understood (26). We observed a marked infiltration of neutrophils with metabolic triggers despite low E-selectin levels. In accordance with our observations, adhesion of neutrophils within liver sinusoids is thought to be independent of selectins and differs fundamentally from other tissues (26). The activation of AP-1 may explain why metabolic inflammatory triggers stimulate neutrophil recruitment: the main chemoattractants for neutrophils in mice, keratinocyte cytokine (KC)(CXCL-8/IL-8 in humans) and macrophage inflammatory protein-2 (MIP-2), are transcriptionally regulated by NFκB *and* AP-1 (27). Transcription of MIP-2 depends on a simultaneous activation of both transcription factors, i.e. a condition that was achieved with two metabolic triggers in the present study but was absent in the case of the two non-metabolic triggers. Further support for a crucial role of the AP-1 signaling pathway in NASH comes from knock-out studies: phosphorylation of the AP-1 subunit c-Jun is diminished in Jnk1-deficient mice and these mice show a reduced development of steatohepatitis (28).

Of note, the two metabolic triggers induced different factors that are known to be risk factors for NASH in humans, i.e. adiposity/insulin resistance (carbohydrate) and dyslipidemia (cholesterol). This suggests that the pathogenic processes leading to liver damage, neutrophil infiltration and AP-1 activation may differ between these triggers. Because plasma levels of HDL were reduced by both metabolic as well as non-metabolic triggers, it is unlikely that HDL has a major role in the pathogenic processes mediating the transition from steatosis to NASH. Our data also do not indicate a major role for the inflammatory pathways leading to activation of STAT3 or C/EBP-β.

Treatment with inflammatory stimuli was started once steatosis was already manifest (after 10 weeks of HFD feeding) and reportedly still reversible (29), in order to mimic a risk population with established steatosis (21, 30). HFD feeding alone causes metabolic stress and renders livers susceptible to injury (13, 20) and the superimposed insults represent ‘second hits’. Importantly, feeding of a HFD alone only resulted in a steatotic liver within the study period and did not cause NASH or cellular inflammation. This has also been observed in other HFD-feeding studies of comparable lengths of time using diets with similar content of fat, i.e. ≤25% w/w. This equals about 45% energy from fat (20) which is reached in human diets in Finland and Crete (31). Of note, experimental diets that contain very high, supraphysiological quantities of fat (e.g. >50% energy) as well as experimental diets deficient in methionine and choline (MCD diets) may develop a more severe and different liver pathology. The translational character of such studies is debated because MCD-fed mice lose weight due to a vastly lower caloric intake and do not become insulin resistant while most humans with NASH are obese and insulin resistant (1-3).

It is generally assumed that chronic activation of NFκB in the liver is a main driver of the transition from BS to NASH. In the present study we compared different NFκB-inducing inflammatory triggers (head-to-head and superimposed on HFD) regarding their ability to induce this transition to NASH. We observed that activation of NFκB in the liver *per se* (upon stimulation with LPS or IL-1β) does not promote a transition from BS to NASH. By contrast, metabolic inducers of inflammation like cholesterol and carbohydrate had a greater ability to induce a human NASH-like phenotype. This suggests that chronic inflammation caused by metabolic triggers activates additional inflammatory pathways and biological processes than LPS or IL-1β. To our knowledge, this is the first study that compares metabolic inflammatory triggers (high carbohydrate, cholesterol) to non-metabolic (classical) inflammatory chronic triggers (LPS, IL-1β) in a head-to-head approach, and that defines molecular differences between 'metabolic' and 'non-metabolic' inflammatory triggers. More specifically, we show that metabolic triggers activate AP-1 in the liver and lead to neutrophil infiltration, both of which could be causative factors in the development of NASH. These mechanistic insights as well as the experimental conditions defined herein may help to further elucidate the etiology of NASH and contribute to development of therapeutic strategies directed at attenuating metabolic overload and associated pathologic conditions.

ACKNOWLEDGEMENTS

The authors thank Erik H. Offerman, Niels Kloosterhuis, José van der Hoorn, Adri Mulder, Karin Toet and Simone van der Drift-Droog for technical assistance. This research was performed within the framework of CTMM, the Center for Translational Molecular Medicine (www.ctmm.nl), project PREDICCt (grant 01C-104), and supported by the Dutch Heart Foundation, Dutch Diabetes Research Foundation and Dutch Kidney Foundation.

REFERENCES

1. Bellentani S, Marino M. Epidemiology and natural history of non-alcoholic fatty liver disease (NAFLD). Ann Hepatol 2009;8 Suppl 1:S4-8.

2. Edmison J, McCullough AJ. Pathogenesis of non-alcoholic steatohepatitis: Human data. Clin Liver Dis 2007;11(1):75,104, ix.

3. Lazo M, Clark JM. The epidemiology of nonalcoholic fatty liver disease: A global perspective. Semin Liver Dis 2008;28(4):339-50.

4. Fujii H, Kawada N. Inflammation and fibrogenesis in steatohepatitis. J Gastroenterol 2012;47(3):215-25.

5. Harmon RC, Tiniakos DG, Argo CK. Inflammation in nonalcoholic steatohepatitis. Expert Rev Gastroenterol Hepatol 2011;5(2):189-200.

6. Nomura K, Yamanouchi T. The role of fructose-enriched diets in mechanisms of nonalcoholic fatty liver disease. J Nutr Biochem 2012;23(3):203-8.

7. Wieckowska A, Feldstein AE. Diagnosis of nonalcoholic fatty liver disease: Invasive versus noninvasive. Semin Liver Dis 2008;28(4):386-95.

8. Cai D, Yuan M, Frantz DF, et al. Local and systemic insulin resistance resulting from hepatic activation of IKK-beta and NF-kappaB. Nat Med 2005;11(2):183-90.

9. Ruiz AG, Casafont F, Crespo J, et al. Lipopolysaccharide-binding protein plasma levels and liver TNF-alpha gene expression in obese patients: Evidence for the potential role of endotoxin in the pathogenesis of non-alcoholic steatohepatitis. Obes Surg 2007;17(10):1374-80.
10. Nozaki Y, Saibara T, Nemoto Y, et al. Polymorphisms of interleukin-1 beta and beta 3-adrenergic receptor in japanese patients with nonalcoholic steatohepatitis. Alcohol Clin Exp Res 2004;28(8 Suppl Proceedings):106S-10S.
11. Liang W, Tonini G, Mulder P, et al. Coordinated and interactive expression of genes of lipid metabolism and inflammation in adipose tissue and liver during metabolic overload. PLoS One 2013;8(9):e75290.
12. Kleemann R, Verschuren L, van Erk MJ, et al. Atherosclerosis and liver inflammation induced by increased dietary cholesterol intake: A combined transcriptomics and metabolomics analysis. Genome Biol 2007;8(9):R200.
13. Wielinga PY, Yakala GK, Heeringa P, et al. Beneficial effects of alternate dietary regimen on liver inflammation, atherosclerosis and renal activation. PLoS One 2011;6(3):e18432.
14. Vergnes L, Phan J, Strauss M, et al. Cholesterol and cholate components of an atherogenic diet induce distinct stages of hepatic inflammatory gene expression. J Biol Chem 2003;278(44):42774-84.
15. Neuschwander-Tetri BA. Hepatic lipotoxicity and the pathogenesis of nonalcoholic steatohepatitis: The central role of nontriglyceride fatty acid metabolites. Hepatology 2010;52(2):774-88.
16. Bijland S, van den Berg SA, Voshol PJ, et al. CETP does not affect triglyceride production or clearance in APOE*3-leiden mice. J Lipid Res 2010;51(1):97-102.
17. Westerterp M, van der Hoogt CC, de Haan W, et al. Cholesteryl ester transfer protein decreases high-density lipoprotein and severely aggravates atherosclerosis in APOE*3-leiden mice. Arterioscler Thromb Vasc Biol 2006;26(11):2552-9.
18. Lindeman JH, Abdul-Hussien H, van Bockel JH, et al. Clinical trial of doxycycline for matrix metalloproteinase-9 inhibition in patients with an abdominal aneurysm: Doxycycline selectively depletes aortic wall neutrophils and cytotoxic T cells. Circulation 2009;119(16):2209-16.
19. Kleiner DE, Brunt EM, Van Natta M, et al. Design and validation of a histological scoring system for nonalcoholic fatty liver disease. Hepatology 2005;41(6):1313-21.
20. Kleemann R, van Erk M, Verschuren L, et al. Time-resolved and tissue-specific systems analysis of the pathogenesis of insulin resistance. PLoS One 2010;5(1):e8817.
21. Hubscher SG. Histological assessment of non-alcoholic fatty liver disease. Histopathology 2006;49(5):450-65.
22. Van Rooyen DM, Gan LT, Yeh MM, et al. Pharmacological cholesterol lowering reverses fibrotic NASH in obese, diabetic mice with metabolic syndrome. J Hepatol 2013.
23. Lassenius MI, Pietilainen KH, Kaartinen K, et al. Bacterial endotoxin activity in human serum is associated with dyslipidemia, insulin resistance, obesity, and chronic inflammation. Diabetes Care 2011;34(8):1809-15.
24. Westerterp M, Berbee JF, Pires NM, et al. Apolipoprotein C-I is crucially involved in lipopolysaccharide-induced atherosclerosis development in apolipoprotein E-knockout mice. Circulation 2007;116(19):2173-81.
25. Rensen SS, Slaats Y, Nijhuis J, et al. Increased hepatic myeloperoxidase activity in obese subjects with nonalcoholic steatohepatitis. Am J Pathol 2009;175(4):1473-82.
26. Kubes P, Mehal WZ. Sterile inflammation in the liver. Gastroenterology 2012;143(5):1158-72.
27. Orlichenko LS, Behari J, Yeh TH, et al. Transcriptional regulation of CXC-ELR chemokines KC and MIP-2 in mouse pancreatic acini. Am J Physiol Gastrointest Liver Physiol 2010;299(4):G867-76.
28. Singh R, Wang Y, Xiang Y, et al. Differential effects of JNK1 and JNK2 inhibition on murine

steatohepatitis and insulin resistance. Hepatology 2009;49(1):87-96.
29. Radonjic M, Wielinga PY, Wopereis S, et al. Differential effects of drug interventions and dietary lifestyle in developing type 2 diabetes and complications: A systems biology analysis in LDLr-/- mice. PLoS One 2013;8(2):e56122.
30. Brunt EM. Pathology of nonalcoholic fatty liver disease. Nat Rev Gastroenterol Hepatol 2010;7(4):195-203.
31. Hu FB, Manson JE, Willett WC. Types of dietary fat and risk of coronary heart disease: A critical review. J Am Coll Nutr 2001;20(1):5-19.

SUPPLEMENTARY DATA

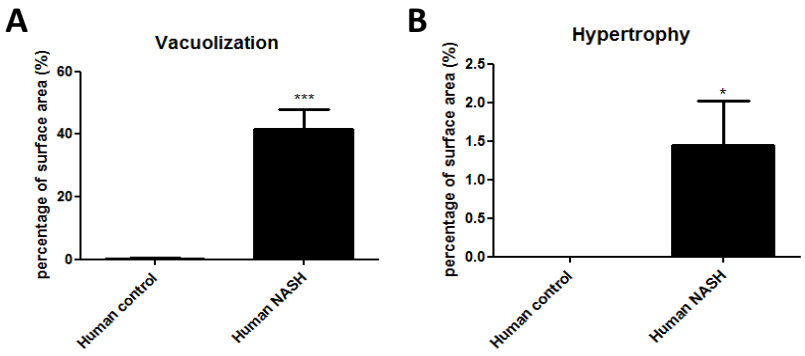

Supplemental Figure A/B: Histological quantification of vacuolization (A) and hepatocellular hypertrophy (B). The percentage of A) vacuolization (micro- and macrovacuolization) and B) hypertrophic cells was analyzed in human liver sections. Hepatocellular hypertrophy is defined as enlargement of hepatocytes (>1.5 normal diameter) and characterized by small lipid droplets in the cytoplasm of the hepatocytes.
Values are means ± SEM. ***P≤0.001 indicates statistical significance between human control livers and NASH livers tested by Mann-Whitney test. *P≤0.05 indicates statistical significance between human control livers and NASH livers tested by Wilcoxon matched-pairs signed rank test. Wilcoxon testing was used because hypertrophy was absent in all control livers.

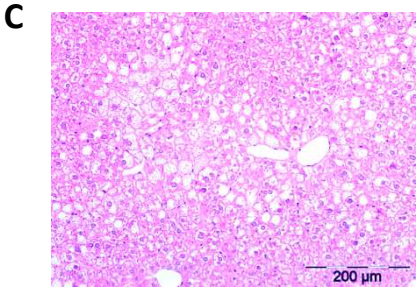

Supplemental Figure C: Histological presentation of steatosis in ApoE*3L.CETP mice after 10 weeks of HFD feeding (end of run-in). Animals developed simple steatosis during the run-in period on HFD. This condition defines the start of the intervention with inflammatory triggers.

D

Supplemental Figure D: Histological analysis of individual mice and their NASH pathology. The first column specifies the experimental groups and rows represent individual mice. Livers (two cross-sections per animal) were analyzed for centrilobular vacuolization (CHV), midzonal vacuolization (MHV), periportal vacuolization (PHV), hepatocellular hypertrophy (HHP) and inflammatory cell clusters (foci). Depending on the type of inflammatory cells in a cluster, a distinction was made between mononuclear inflammatory cell clusters (MNC) and mixed-type (mononuclear and polymorph) nuclear cell clusters (MIC). The color code (from green to red) represents the severity of a parameter as indicated in the columns at the right.

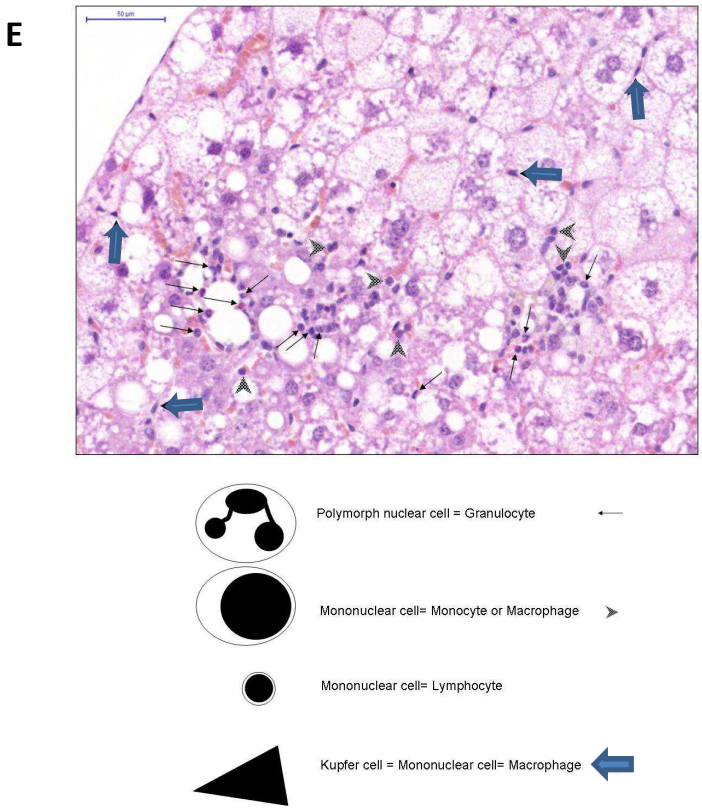

Supplemental Figure E: Histological presentation of a mouse liver with NASH (as a reference). The different inflammatory cells present in NASH (polymorph nuclear cell; monocyte/macrophage; lymphocyte and Kupfer cells) are indicated with arrows as specified above. These hallmarks of inflammation were not found after 10 weeks of HFD feeding in ApoE*3L.CETP mice (end of run-in).

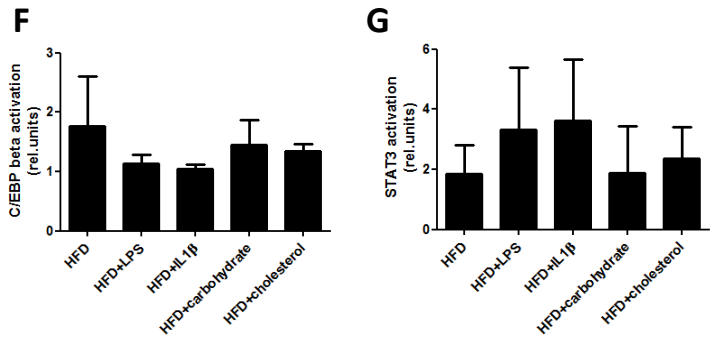

Supplemental Figure F/G: Activity of transcription factors C/EBP-β and STAT3 using TransAM® analysis. There were no significant differences between the experimental groups. Values are means ± SEM.